



Isotopic apportionment of sulfate aerosols between natural and anthropogenic sources in the outflow of South Asia

Sean Clarke¹, Henry Holmstrand¹, Krishnakant Budhavant^{2,3}, Manoj Remani¹, Sophie Haslett¹, Katerina Rodiouchkina^{4,5}, Ellen Kooijman⁶, and Örjan Gustafsson¹

¹Department of Environmental Science, Stockholm University, 11418 Stockholm, Sweden

²Maldives Climate Observatory at Hanimaadhoo, H. Dh. Hanimaadhoo, Maldives

³Divecha Centre for Climate Change, Indian Institute of Science, Bangalore, Karnataka 560012, India

⁴Division of Geosciences, Luleå University of Technology, 971 87 Luleå, Sweden

⁵ALS Scandinavia AB, 977 75, Luleå, Sweden

⁶Department of Geosciences, Swedish Museum of Natural History, Box 50 007, 104 05 Stockholm, Sweden

Correspondence: Sean Clarke (sean.clarke@aces.su.se) and Örjan Gustafsson (orjan.gustafsson@aces.su.se)

Received: 28 October 2025 – Discussion started: 1 December 2025

Revised: 11 March 2026 – Accepted: 20 March 2026 – Published: 21 April 2026

Abstract. Sulfate aerosols cool the climate and thus temporarily mask climate warming, but at a cost to air quality. Their short atmospheric lifetime leads to heterogeneous global coverage, with sulfate concentrations over South Asia being especially elevated and continuing to increase. It remains challenging to constrain the relative importance of different emission sources due to poor observational coverage and uncertainties in bottom-up technology-based emission estimates. The stable sulfur isotope composition ($\delta^{34}\text{S-SO}_4^{2-}$) quantitatively distinguishes natural and anthropogenic sources. This study aimed to constrain the sources of sulfate arriving at the Maldives Climate Observatory Hanimaadhoo (MCOH), which is ideally situated for intercepting the outflow from airsheds over the Indian subcontinent. The results show that anthropogenic sources of sulfate contributed $93 \pm 14\%$, $87 \pm 10\%$, and $66 \pm 12\%$ in winter (post-monsoon), spring (pre-monsoon), and summer (monsoon), respectively. There was also a moderate to strong correlation ($r^2 = 0.75$, $p \ll 0.05$, $n = 7$) between continental anthropogenic (winter and spring) sulfate ($\delta^{34}\text{S}$) and black carbon aerosols from fossil fuel combustion (pinpointed by $\Delta^{14}\text{C}$). This study provides improved constraints on sulfate sources for South Asia – a key region for aerosol pollution and aerosol masking of climate warming.

1 Introduction

Anthropogenic aerosols cause substantial net negative climate forcing, which is currently attenuating the warming caused by the emissions of greenhouse gases. Sulfate aerosols represent the largest component of this aerosol-induced masking of climate warming and the health-affecting deterioration of air quality. Sulfate aerosols are primarily secondary aerosols formed from the oxidation (via H_2O_2 , O_3 , OH, transition metals, NO_2) of sulfur dioxide, hydrogen sulfide, and sulfur-bearing organic substances, emitted from numerous natural and anthropogenic sources (e.g., Berresheim

et al., 2002; Szopa et al., 2021). These aerosols then alter the climate through the direct (scattering of light) and indirect effects (primarily alteration of cloud properties), leading to a net cooling effect (e.g., Charlson et al., 1991; Szopa et al., 2021).

These climatic effects are associated with the ubiquitous presence of sulfate aerosols in the atmosphere, leading to an effective radiative forcing (ERF) of -0.94 Wm^{-2} [-1.63 to -0.25 Wm^{-2}] (Szopa et al., 2021). However, the aerosols' short atmospheric lifetime (1–2 weeks) is expected to lead to a rapid readjustment once emissions change.

There have been regional reductions in sulfate emissions in North America and Europe for several decades. While these reductions are significant environmental legislative successes, emission patterns shifted eastwards towards Asia. The rise in emissions in East Asia led to a brief increase in global emissions at the start of the 21st century (McDuffie et al., 2020). However, subsequent successful mitigation efforts primarily in China have dramatically decreased sulfate loadings in the recent decade (McDuffie et al., 2020). The emissions from India surpassed those of China at the end of the last decade (Li et al., 2017); South Asia is currently the epicenter of sulfate emissions, with emissions still believed to be on the rise (McDuffie et al., 2020).

South Asia experienced rapid industrialization and economic growth in the latter part of the 20th century that have continued into the present day, with the unintended consequence of high aerosol emissions. These loadings are shown by the increasing trend over the last few decades in the aerosol optical depth (AOD), with sulfate being a large contributor to this increase (Aas et al., 2019; Gupta et al., 2023). These high aerosol loadings must be addressed as they are a major health and environmental burden on South Asia, which is home to almost a quarter of the world's population (Lelieveld et al., 2020). However, our knowledge about sulfate sources and emissions remains uncertain with notable disparities between estimates from emission inventories and from remote sensing (Elguindi et al., 2020; Sharma and Kumar, 2016). The understanding of sulfate emissions is further hampered by uncertainties in natural emissions, such as oceanic dimethyl sulfide (DMS), which has seasonal and regional emission fluctuations ranging by a factor of 10–100 (Norman et al., 1999, 2004; Shenoy and Kumar, 2007). These uncertainties lead to large variations in estimates of natural versus anthropogenic contributions, especially in locations surrounded by oceans such as South Asia (Norman et al., 1999, 2004; Shenoy and Kumar, 2007). Quantitative top-down source-diagnostic isotopic composition, in combination with consideration of air-mass origins, presents an opportunity to quantitatively apportion the relative contributions from anthropogenic and natural sources of sulfate for the wider receptor atmosphere of South Asia.

Isotopic composition allows for the quantitative separation of natural versus anthropogenic sources of sulfate through distinct source end-member compositions (source fingerprints). The use of $\delta^{34}\text{S}$ for separating natural vs. anthropogenic sources is established, with a few pioneering studies now also in South Asia (Dasari and Widory, 2024; Rastogi et al., 2020; Sawlani et al., 2019).

This study employs isotopic $\delta^{34}\text{S}$ source apportionment of SO_4^{2-} to quantify the anthropogenic sulfate contributions to the expansive airshed outflow from South Asia (representative of the wider system of the regional aerosol-climate effect). The present study has a much wider footprint and longer time coverage than earlier studies in the region. Distinguishing the relative source contributions of the

climate-affecting sulfate in the South Asia region provides guidance for future mitigation strategies and also provides observation-based constraints useful for climate models.

2 Methods

2.1 Site description and meteorological context

South Asia encompasses several climate zones with its climate being primarily driven by the South Asian monsoon. The monsoon season marks the onset of frequent precipitation events and the reversal of the prevailing northerly winds. The southerly monsoon winds transport air masses from the Indian Ocean to the continent. Seasonal oscillation also occurs in the zonal (east-west) wind component, with stronger easterlies during winter and autumn (from the Bay of Bengal), and more westerly flow in spring (from the Arabian Sea).

Meteorologically, this leads to air masses from the high-emission region of the Indo-Gangetic Plain (IGP) being transported into the Bay of Bengal in winter/autumn with dispersal of their anthropogenic load also over the northern Indian Ocean (see Fig. 1). The IGP is a fertile, densely populated and highly industrialized region spanning several countries. The IGP contributes the highest aerosol loading in South Asia and strongly impacts aerosol loadings far out over the Indian Ocean (Aswini et al., 2020; Nair et al., 2023; Ramanathan et al., 2001; Verma et al., 2012).

The Maldives Climate Observatory at Hanimaadhoo (MCOH; $6^\circ 46' 34''$ N, $73^\circ 10' 59''$ E; tower inlet at 15 m a.g.l.) is ideally situated for intercepting air masses arriving from the polluted and polluting IGP, the subcontinent at large, and additionally from the open Indian Ocean during the summer (see Fig. 1). As the IGP is the key source region of anthropogenic aerosols, two additional sites were chosen in this emission region to constrain its anthropogenic sulfate signature. These sites were the Delhi branch of the Indian Institute of Tropical Meteorology (IITM-Delhi; $28^\circ 35' \text{ N}$, $77^\circ 12' \text{ E}$; 15 m a.g.l.) and the Bangladesh Climate Observatory Bhola (BCOB; $22^\circ 17' 00'' \text{ N}$, $90^\circ 42' 36'' \text{ E}$, 10 m a.g.l.) (see Fig. 1). Detailed information on the observatory sites can be found in previous studies (e.g., Bikkina et al., 2019; Dasari et al., 2019).

2.2 Collection of aerosols

Samples for stable sulfur isotope measurements of sulfate in this study were hence collected from three sites in South Asia. The urban $\text{PM}_{2.5}$ filters (47 mm diameter quartz filters, Millipore) were collected from the IITM-Delhi in the winter of 2016 (January and February) using a high-volume sampler (APM 550 Envirotech, flow rate = $1 \text{ m}^3 \text{ h}^{-1}$, time = 12 h). The IGP outflow $\text{PM}_{2.5}$ filters were collected at BCOB in the winter of 2016 (January), using a high-volume sampler (model DH77, DIGITEL A.G., Switzerland, flow

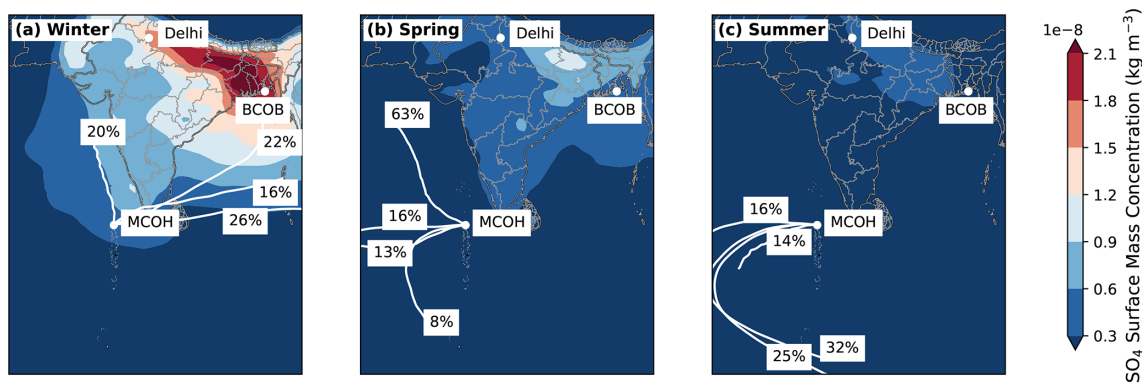


Figure 1. Remote sensing estimates of sulfate surface concentration (MERRA-2) and average back trajectories (7 d clusters; HYSPLIT, white lines depict the mean paths of the HYSPLIT back-trajectory clusters) for South Asia, for three seasons: (a) winter (December–March 2015–2016); (b) spring (April–May 2013); (c) summer (June–September 2015).

rate = 500 L min^{-1} , time = 24 h). The integrating filters of the South Asian outflow, intercepted over the Indian Ocean, were collected at MCOH with sample dates spanning several years (winter = 2016, summer = 2013–2015, spring = 2013) (winter = PM_{10} , spring and summer = $\text{PM}_{2.5}$) using a high-volume sampler (model DH77, DIGITEL A.G., Switzerland, flow rate = 500 L min^{-1} , time = 24 h). Detailed information on the collection of aerosol samples can be found in previous studies (e.g., Kirillova et al., 2013, 2014).

2.3 Ionic concentrations

Ionic concentrations (Cl^- , Br^- , NO_2^- , NO_3^- , PO_4^{3-} , SO_4^{2-} , Na^+ , NH_4^+ , K^+ , Mg^{2+} , Ca^{2+}) were measured using a Dionex Aquion ion chromatography (IC) system (Thermo Finnigan LLC, Dionex IonPac CS12A) anion (Dionex IonPac AS22 fast). Cut-outs ($1\text{--}4 \text{ cm}^2$) of the filter samples were dissolved in 10 mL of Milli-Q water and analyzed with a flow rate of 1 mL min^{-1} . Standards and field blanks were used to ensure quality control and minimize external influences.

The sea spray fraction of SO_4^{2-} was removed following (Keene et al., 1986), as shown in Eq. (1):

$$\text{nss-}\text{SO}_4^{2-} = \left[\text{SO}_4^{2-} \right] - \left(\frac{\left[\text{SO}_4^{2-} \right]}{\left[\text{Na}^+ \right]} \right)_{\text{sea}} \times \left[\text{Na}^+ \right] \quad (1)$$

The $\text{nss-}\text{SO}_4^{2-}$ is the non-sea salt sulfate, with the mass ratio of sulfate to sodium from sea water being 0.253 taken from (Keene et al., 1986). Seawater is enriched in sulfate due to long-term accumulation. This results in natural emissions of sulfate aerosols from sea spray, which must be accounted for to enable accurate source apportionment of $\text{nss-}\text{SO}_4^{2-}$.

2.4 Isotopic analysis

2.4.1 Analysis of $\delta^{34}\text{S}$

The determination of the $\delta^{34}\text{S}$ composition of aerosols on 17 carefully selected samples was performed following the method described in detail in Rodiouchkina (2018). Filter cut-outs were placed in polypropylene tubes and Milli-Q water was added to extract the sulfate (5 h in an ultrasonic bath). Sulfur was then isolated using anion exchange chromatography (AG 1-X8, analytical grade, 200–400 mesh, chloride form, Bio-Rad Laboratories, USA). The standards (S1, S3, and S4 from IAEA, Austria) and samples were then diluted to an S concentration of $2 \mu\text{g mL}^{-1}$ before being run in a solution matrix of 0.3 M HNO_3 (sub-boiled). Silicon (Si) was added to all solutions as ammonium hexafluorosilicic acid ($(\text{NH}_4)_2\text{SiF}_6$), at a concentration ratio of 1 : 1 (S : Si, $\mu\text{g mL}^{-1}$: $\mu\text{g mL}^{-1}$) for internal standardization. Additionally, sodium (Na) was added as sodium carbonate (Na_2CO_3) at a molar ratio of 2 (Na / S) to all measurement solutions. The measurements were carried out using a multi-collector inductively coupled plasma mass spectrometer (MC-ICP-MS, Nu Plasma II, Nu Instruments, UK) and run in dry plasma mode using a desolvator (Aridus II, CETAC, USA) at the Vegacenter facility of the Swedish Museum of Natural History, Stockholm, Sweden. Detailed descriptions and typical operating parameters can be found in Rodiouchkina (2018). For instrument settings and parameters, see Sect. S1 in the Supplement.

2.4.2 Analysis of radiocarbon ($\Delta^{14}\text{C}$) composition in Black Carbon (BC)

A total of 14 samples for $\Delta^{14}\text{C}$ were prepared for dual isotopic analysis of combustion-derived BC (MCOH spring = 2, MCOH summer = 3, BCOB = 3, MCOH winter = 6). The winter samples comprise data taken from Dasari et al. (2020). Inorganic carbonates were removed by acid fumi-

gation (12 M HCl) for 24 h, then the samples were dried at 60 °C for 1 h. The samples were subjected to thermal-oxidation separation of OC from BC using a TOT analyzer (Thermal Optical Transmittance, Sunset Laboratory, Tigard, Oregon, USA) and the resulting carbon dioxide derived from the BC fraction was trapped using a custom-built system described and extensively tested earlier (e.g., Andersson et al., 2015; Chen et al., 2013; Winiger et al., 2015). The trapped CO₂ from the BC fraction was then sent to the collaborating Accelerator Mass Spectrometry facility (AMS) at Uppsala University (Sweden) for $\Delta^{14}\text{C}$ isotopic analysis. The source apportionment was calculated using Eqs. (2) and (3), with end-member values taken from the literature (Andersson et al., 2015; Bikkina et al., 2019).

$$\Delta^{14}\text{C}_{\text{BC}} = \left[F_m \times e^{\frac{-(\text{year}-1954)}{8267}} - 1 \right] \times 1000 \quad (2)$$

$$\Delta^{14}\text{C}_{\text{BC}} = \Delta^{14}\text{C}_{\text{biomass}} \times F_{\text{bio-BC}} + \Delta^{14}\text{C}_{\text{fossil}} \times (1 - F_{\text{bio-BC}}) \quad (3)$$

2.5 Model for apportioning between natural and anthropogenic sulfur input

The approach to apportion natural versus anthropogenic sulfate was carried out in several steps. First, the data were corrected for the minor contribution from sea spray based on the well-known isotopic composition of sea water using Eq. (4). The sample MCOH PM_{1-13-14/01/2016} was corrected using the fraction of non-sea salt contribution to tot-SO₄ from the other samples (98.9 ± 0.2 %) due to sample depletion.

$$\delta^{34}\text{S}_{\text{nss}} = \left(\delta^{34}\text{S} - \left(\frac{100 - F_{\text{nssSO}_4}}{100} \right) \times \delta^{34}\text{S}_{\text{sea water}} \right) / \frac{\% \text{nssSO}_4}{100} \quad (4)$$

The isotopic composition of $\delta^{34}\text{S}_{\text{sea water}}$ is +21 ± 0.2 ‰ from Böttcher et al. (2007) and Rees et al. (1978). The percentage of nss-SO₄²⁻ is determined from Eq. (1).

After this correction, the nss- $\delta^{34}\text{S}$ was used in a binary model to apportion the relative contributions from anthropogenic-fossil sources (e.g., ship emissions/IGP sources) vs. the marine biogenic (DMS) source, using Eq. (5):

$$\delta^{34}\text{S}_{\text{nss}} = \delta^{34}\text{S}_{\text{DMS}} \times F_{\text{DMS-SO}_4} + \delta^{34}\text{S}_{\text{anthropogenic}} \times (1 - F_{\text{DMS-SO}_4}) \quad (5)$$

where F represents the fraction (DMS and anthropogenic), $\delta^{34}\text{S}_{\text{nss}}$ represents the $\delta^{34}\text{S}$ of the sample, $\delta^{34}\text{S}_{\text{DMS}}$ and $\delta^{34}\text{S}_{\text{anthropogenic}}$ refer to the mean isotopic composition of the end-members (DMS and anthropogenic). The DMS end-member was taken from Amrani et al. (2013), with a $\delta^{34}\text{S}$ composition of +18.8 ± 0.5 ‰. The anthropogenic end-member varies by season and is constrained by a combination of literature reports and new findings in this study.

For samples where air masses originated from the continent (spring, winter), an IGP end-member was used. The IGP end-member had a $\delta^{34}\text{S}$ of 2.3 ± 1.7 ‰ calculated from this study and literature (Dasari and Widory, 2024; Sawlani et al., 2019, Supplement Table S1). The ship end-member had a $\delta^{34}\text{S}$ of 3 ± 3 ‰ taken from studies that measured $\delta^{34}\text{-SO}_4$ and $\delta^{34}\text{-SO}_2$ in the North Atlantic, which is thought to be representative of remote air masses with strong ship emissions from heavy fuel oil (Seguin et al., 2010, 2011; Wadleigh, 2004).

2.6 Satellite imagery and computational analysis

The Hybrid Single-Particle Lagrangian Integrated Trajectory (HYSPLIT) model was used to run 7 d backward trajectories from the NOAA Air Research Laboratory (available at <http://ready.arl.noaa.gov/HYSPLIT.php>, last access: June 2025). Back trajectories for seasonal clusters were calculated for summer (June–September 2015), winter (December–March 2015–2016) and spring (April–May 2015).

MERRA-2 (Modern-Era Retrospective Analysis for Research and Applications, version 2) and TROPES (TROPOspheric Ozone and its Precursors from Earth System Sounding) were used to retrieve model-estimated surface concentrations of black carbon and sulfate. MERRA-2 is a reanalysis product that uses remote sensing aerosol optical depth (satellite- and ground-based) in combination with the Goddard Earth Observing System Model, Version 5 to calculate aerosol concentrations (Buchard et al., 2017; Gelaro et al., 2017; Randles et al., 2017). TROPES includes additional satellite measurements (TES, AIRS, TROPOMI, and OMPS) combined with a retrieval algorithm to obtain sulfate surface concentrations (Miyazaki, 2024).

2.7 Emission inventory

The Community Emissions Data System (CEDSV2021_04_21) is a bottom-up emission inventory that provides gridded and national fluxes of short-lived climate pollutants (Hoesly et al., 2018). The national inventory dataset is available at <https://doi.org/10.25584/PNNLDataHub/1779095> (PNNL, 2026).

3 Results and discussion

3.1 Constraints on isotopic signatures of different sources

Reports on the isotopic composition of sulfate from different sources and regions display a large range, although marine natural sources are clearly enriched in ³⁴S compared to anthropogenic sources. Natural sources considered in this study were sea spray and dimethyl sulfide (DMS), the dominant marine biogenic source. Sea spray and DMS have a well-defined isotopic composition of +21 ± 0.2 ‰ and

+19.7 ± 0.5 ‰, respectively (Amrani et al., 2013; Böttcher et al., 2007; Rees et al., 1978). In contrast, fossil fuel end-members can vary (−35 ‰ to +33 ‰) depending on fuel type (liquid vs. solid), as well as having strong geographical differences (Jongebloed et al., 2023; Lee et al., 2023). Additional details on sulfate sources and considerations in sulfur-isotopic attribution studies are provided in Sect. S2.

To account for the potential variability in fossil fuel isotope end-members, an anthropogenic end-member was determined through sampling in the regional source-integrating air masses of the IGP, with end-member uncertainty accounted for through error propagation (Sect. S3). The samples were first split based on air mass origin into a continental anthropogenic end-member and an oceanic anthropogenic end-member. The oceanic anthropogenic input was expected to be predominantly from ship emissions, with a $\delta^{34}\text{S}$ signature of 3 ± 3 ‰ taken from the literature on the marine anthropogenic end-member (Seguin et al., 2010, 2011; Wadleigh, 2004, Sect. S2). The oceanic anthropogenic and continental anthropogenic end-members were treated as distinct to reflect their different origins. Ship emissions may contribute to the continental end-member, but available top-down (MERRA-2) and bottom-up (CEDS) constraints indicate that these contributions are much smaller than land-based continental emissions (Buchard et al., 2017; Randles et al., 2017; Hoesly et al., 2018). In any case, the choice of end-member changes the inferred anthropogenic contribution by at most ~ 3 ‰.

The integrated continental anthropogenic signature was calculated directly from $\delta^{34}\text{S}$ (SO_4^{2-}) measured on aerosol filters in the IGP (Delhi and COB), with samples measured in this study and from the literature, resulting in an end-member value of 2.3 ± 1.7 ‰ (see Fig. 2, Table S1; Dasari and Widory, 2024; Sawlani et al., 2019, $n = 50$). Analysing source aerosols captures isotope fractionation during SO_2 oxidation to sulfate, which can be substantial (≈ 3 ‰ enrichment in urban environments, Sect. S2; Lee et al., 2023). The IGP end-member in this study was assumed to be predominantly anthropogenic. Potential crustal and biogenic contributions are expected to be minor (Dasari and Widory, 2024). Our sensitivity analysis shows that including a 5%–10% non-anthropogenic sulfate fraction does not change the source apportionment beyond the propagated uncertainty (Sect. S4, Table S2). We also investigated the use of a Keeling plot to determine the anthropogenic end-member, but did not apply this approach because mixed and variable sources could bias the inferred end-member toward depleted values (Sect. S5 and Fig. S1 in the Supplement). The average from this study was slightly lower due to one sample showing a near-zero $\delta^{34}\text{S}$ value (−0.07 ‰). This $\delta^{34}\text{S}$ -depleted sample likely reflects sulfate formation through oxidation catalyzed by transition metal ions (TMI) and is associated with poor air quality, reported during hazy conditions (Harris et al., 2013; Sawlani et al., 2019). Alternatively, this type of isotope depletion has been proposed to be related to increased coal in-

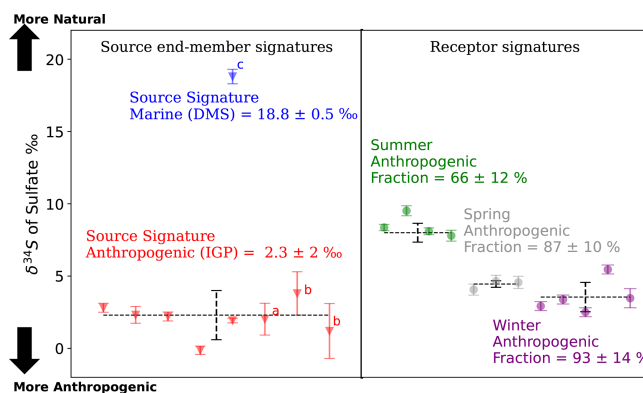


Figure 2. Sulfate $\delta^{34}\text{S}$ composition for MCOH and end-members: IGP source signature (this study, $n = 5$; a = Dasari and Widory, 2024, $n = 15$; b = Sawlani et al., 2019, $n = 30$), DMS source signature (blue; c = Amrani et al., 2013, $n = 16$). MCOH summer (green), spring (grey), and winter (purple). Error bars for this study's samples show $\pm 4\sigma$ (instrumental analytical precision, per measurement). Literature points and seasonal aggregates show $\pm 2\sigma$ (between-sample standard deviation).

put or terrigenous sulfate (Dasari and Widory, 2024). These depleted oxidative pathways/sources are likely to occur as a continuum, motivating the inclusion of the depleted sample.

3.2 Abundance of sulfate aerosols over the northern Indian Ocean

There are only limited reports of measured sulfate concentrations over the Indian Ocean, an area integral to South Asia's monsoon/hydrological cycles and aerosol-affected regional climate forcing. This reduces the confidence in our understanding of the regional loadings of sulfate and the effective regional climate forcing. The loadings for the non-sea salt sulfate (nss-SO_4^{2-}) over the northern Indian Ocean for winter, spring, and summer in this study were $10 \pm 4 \mu\text{g m}^{-3}$ ($96 \pm 6\%$ nss-SO_4^{2-} , full period $n = 43$ from Dasari et al., 2019), $5.5 \pm 1 \mu\text{g m}^{-3}$ ($98.5 \pm 0.1\%$ nss-SO_4^{2-}), $1 \pm 0.2 \mu\text{g m}^{-3}$ ($85.5 \pm 5.5\%$ nss-SO_4^{2-}), respectively, with these values broadly agreeing with previous reports from the MCOH receptor of the South Asian outflow (Budhavant et al., 2023, 2024).

Seasonal differences are due to both fluctuating emissions and varying seasonal air transport from the source regions (Fig. 1). These meteorological factors (wind speed, boundary layer height, humidity, etc.) cause winter conditions to be favorable for long-range aerosol transport from the polluted IGP out over the northern Indian Ocean (Aswini et al., 2020; Dasari et al., 2019; Kesti et al., 2020; Ram et al., 2012). With a shortage of in situ measurements, estimates from remote sensing provide a picture of sulfate loadings for remote regions; expansion of in situ atmospheric observatory measurements is critical to the validation of the accuracy of derived estimates from remote sensing.

Remote sensing estimations of sulfate loadings are commonly derived from optical measurements of columnar data, which can differ greatly from ground conditions. The indirect estimates of sulfate surface loadings from remote sensing (MERRA-2, TROPES at $p = 1000$ hPa) were 2–5 times lower than the in situ sulfate measurements in this study (see Fig. S2). These discrepancies need to be confirmed by forthcoming longer and more complete in situ measurement records of sulfate in this critical region for sulfate-climate effects. Long-term in situ records remain pivotal in understanding long-term changes, which become even more valuable when combined with additional analysis such as isotopic source apportionment.

3.3 Source-diagnostic isotopic composition of sulfate aerosols over the northern Indian Ocean

Refined constraints on sulfate sources improve our understanding of the atmospheric cycle of climate-forcing anthropogenic sulfate over South Asia. The study results show that anthropogenic sulfate dominated in the South Asian outflow intercepted over the northern Indian Ocean, yet there is also substantial input of natural sulfate, especially in the monsoon period. The input of anthropogenic sources to the nss-SO_4^{2-} loading was $93 \pm 12\%$, $87 \pm 10\%$, $66 \pm 14\%$ for winter, spring (pre-monsoon), and summer (monsoon), respectively (Fig. 2; Table S1).

These fractions translate into anthropogenic sulfate concentrations of $0.6 \pm 0.2 \mu\text{g m}^{-3}$ (summer), $4.6 \pm 0.7 \mu\text{g m}^{-3}$ (spring) and $9.1 \pm 5 \mu\text{g m}^{-3}$ (samples with $\delta^{34}\text{S}$; winter). Although the summer conditions are cleanest, the region is still highly affected by anthropogenic input, with freight ships during that time likely being an important source. Three major shipping lanes cross the northern Indian Ocean. During the study period, the global shipping emissions were nearly equal to the cumulative emissions of South Asia (McDuffie et al., 2020). These loadings are elevated given the remote location, even with respect to health guidelines for exposure to fine particulate matter.

The World Health Organization (WHO) annual guideline for $\text{PM}_{2.5}$ is $5 \mu\text{g m}^{-3}$ (World Health Organization, 2021), a limit which is frequently exceeded in both winter and spring even this far out over the Indian Ocean, despite local emissions being documented to be low (Budhavat et al., 2015). It is worth noting that a portion of the sulfate loading in the winter air masses from the Bay of Bengal may possibly be influenced by input from mangroves, which emit hydrogen sulfide (H_2S). This gas is rapidly oxidized and typically has a $\delta^{34}\text{S}$ below 0% (Jamieson and Wadleigh, 1999). The H_2S flux from mangroves is potentially significant with emissions estimates ranging from approximately 10%–25% of South Asia's anthropogenic emissions (Ganguly et al., 2018; Hoesly et al., 2018). However, analysis of the back trajectories suggests that sulfate loadings were influenced more by seasonal variation than by specific trajectory pathways (see

Fig. S3). Sulfate loadings reaching MCOH are elevated and are attributed primarily to anthropogenic sources.

This isotope-based source apportionment of sulfate in the receptor-integrated South Asian outflow appears broadly consistent with other regional studies. A study over the northern Bay of Bengal reported $\delta^{34}\text{S} = 4.5 \pm 1.3\%$ in PM_{10} during February–April 2013 (Rastogi et al., 2020). Applying our $\delta^{34}\text{S}$ two-end-member mixing model to those Port Blair PM_{10} values indicates that at least $\sim 90\%$ of sulfate was anthropogenic. This should be viewed as a conservative lower bound because the sea-salt contribution for the isotopic data was not reported (so no sea-salt correction could be applied), and PM_{10} generally contains a larger sea-salt fraction. Similarly, the ICARB-2018 ship campaign estimated anthropogenic sulfate to make up 96% of the nss-SO_4^{2-} in the Arabian Sea and Indian Ocean (Aswini et al., 2020), using the ratio of methanesulfonic acid (MSA) / nss-SO_4^{2-} . These results suggest a quite limited influence of DMS on the total sulfate mass balance over the northern Indian Ocean, even though globally DMS emissions are expected to be a quarter the size of anthropogenic emissions (Lana et al., 2011). These results provide quantitative constraints on sources, showing a strong dominance of anthropogenic sources of sulfate in the northern Indian Ocean, yet with seasonal variations.

3.4 Relationships between sulfate and black carbon

Sulfate precursors and black carbon (BC) are both emitted in large quantities from fossil fuel combustion, yet they also have other separate sources. We explored the extent of co-emission of these two short-lived climate pollutants (SLCPs), having opposing signs in their climate forcing. By comparing isotope-based source indicators ($\delta^{34}\text{S-SO}_4$ and $\Delta^{14}\text{C-BC}$), we observe a positive correlation ($r^2 = 0.75$, $p \ll 0.05$, $n = 7$) between anthropogenic sulfate and the fraction of BC attributed to fossil fuel combustion for the outflow receptor observatory at MCOH (winter and spring) (see Fig. 3 inset). Samples from BCOB, which were used to represent the anthropogenic end-member of sulfate, were assumed to be predominantly anthropogenic in origin ($\sim 100\%$), although minor contributions from dust and biomass are expected (Dasari and Widory, 2024). Summer data were too limited for robust conclusions, although a similar pattern was observed, potentially reflecting differences in emission sources (see Fig. S4). The positive correlation between the isotope fingerprints of these SLCPs lends further credence to the $\delta^{34}\text{S}$ -based findings that fossil fuel combustion is indeed a major source of SO_4^{2-} over South Asia, with additional insight provided by examining the relationship between SO_4^{2-} and climate-warming BC.

Black carbon and sulfate, in part co-emitted, have opposite climatic effects, with BC enhancing climate warming while sulfate masks climate warming. Their opposing climatic effects lead to large uncertainties in radiative forcing due to the ratio of scattering vs. absorbing vectors, espe-

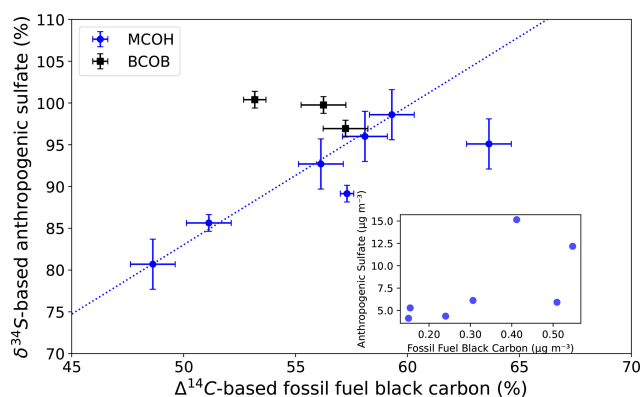


Figure 3. Relationships between fossil fuel black carbon and anthropogenic sulfate for MCOH (spring, summer; blue circles) and BCOB (black squares), calculated using isotopic composition ($\Delta^{14}\text{C}$, $\delta^{34}\text{S}$). The inset graph shows the actual concentrations of fossil fuel black carbon and anthropogenic sulfate for MCOH.

cially in regions with high loadings of both BC and SO_4^{2-} , such as South Asia (Li et al., 2022). The $\text{BC}/\text{SO}_4^{2-}$ ratio for the study period was 0.075 ± 0.03 (spring and winter; summer was excluded due to high variability). The $\text{BC}/\text{SO}_4^{2-}$ ratio in the surface layer estimated from remote sensing by MERRA-2 was much higher for winter during which it was predicted to be 0.16 (2016) and for spring (April 2013) during which it was predicted to be 0.15; both were twice overestimated compared to our direct in situ measurements. The observed $\text{BC}/\text{SO}_4^{2-}$ ratio was compared with an inventory-based BC/SO_2 ratio from the Community Emissions Data System (CEDS v2021-04-21). The BC/SO_2 ratio was obtained by aggregating BC and SO_2 fluxes over India, Pakistan, and Bangladesh. As inventories report SO_2 (not sulfate), BC/SO_2 is used as a proxy for $\text{BC}/\text{SO}_4^{2-}$. The ratio from CEDS was 0.097 (2015–2019 average; Hoesly et al., 2018), which is close to the $\text{BC}/\text{SO}_4^{2-}$ ratio of 0.075 ± 0.03 constrained by in situ measurements in the current study. When we instead compare to the in situ anthropogenic sulfate fraction ($\text{BC}/\text{anthro-SO}_4^{2-}$), the agreement improves (0.082 ± 0.03 ; spring and winter). The uncertainty reflects measurement variability only and does not include additional uncertainty propagated from the $\delta^{34}\text{S}$ end-member constraints. Deviation between emission inventory and in situ may reflect the unaccounted biogenic sulfur inputs (lowering $\text{BC}/\text{SO}_4^{2-}$), while preferential removal of hygroscopic sulfate during transport would act in the opposite direction by increasing $\text{BC}/\text{SO}_4^{2-}$ (e.g., Budhavant et al., 2020). There is a need for increased comparison of $\text{BC}/\text{SO}_4^{2-}$ (and their sources) simulated by models and predicted by emission inventories with greater datasets of in situ observations in South Asia, given the expected changes in their respective emissions and that reduced SO_4^{2-} emissions will unmask current climate warming for the region.

4 Conclusion and outlook

There are very large sulfate loadings over South Asia compared with the global average. However, there is poor spatial coverage of actual measurements of both SO_4^{2-} and its source-diagnostic isotopic composition. This study provides the first multi-seasonal isotope-based source apportionment of sulfate for the integrated outflow airshed of South Asia. The quantitative results show that anthropogenic nss-sulfate is the major contributor to sulfate loadings in this region, yet with clear seasonal and spatial variations and with some contributions also from natural-biogenic sources (e.g., from marine plankton and possibly from mangroves). Quantitative isotope-based observational constraints on the relative contributions of different sources to atmospheric sulfate are vital for both understanding total emissions of this important climate forcer and for guiding strategies to mitigate the anthropogenic components.

Future investigations should aim to constrain the long-term trend (decades) of wintertime and summer sources of sulfate to the South Asian airshed. This will improve the understanding of emission patterns from the heavily polluted IGP, as well as provide potential insights into atmospheric processing due to South Asia's changing meteorology. Aerosol loadings have already been shown to strongly affect the monsoon period (Krishnan et al., 2016; Ramarao et al., 2023). Moreover, both current and past emissions will be needed to understand future changes, with emissions expected to decrease due to socio-economic pressures. Thus, there is an urgent need for improved understanding of all facets of sulfate aerosols to help improve resilience against future climatic impacts, including the extent to which we may need to anticipate enhanced warming (with South Asia being particularly sensitive to heat extremes) due to the demasking of climate warming caused by decreasing sulfate loadings.

Data availability. The datasets generated and analyzed in this study can be accessed from the following link: <https://doi.org/10.17043/clarke-2026-sulfate-aerosols-1> (Clarke et al., 2026). The authors are willing to provide additional information for data that may be of interest to readers upon request.

Supplement. The supplement related to this article is available online at <https://doi.org/10.5194/acp-26-5333-2026-supplement>.

Author contributions. This study was conceptualized by Ö.G. and H.H. Atmospheric sampling strategies and campaign execution were realized by K.B., H.H. and Ö.G. Laboratory procedures, data quality assessments and calculations were performed by M.R., S.C., H.H., K.R. and E.K. Interpretations and the first draft of the manuscript were primarily contributed by H.H., Ö.G., S.C. Finally,

S.C. produced all display items and wrote the manuscript with all authors contributing to detailed data interpretation and writing.

Competing interests. The contact author has declared that none of the authors has any competing interests.

Disclaimer. Publisher's note: Copernicus Publications remains neutral with regard to jurisdictional claims made in the text, published maps, institutional affiliations, or any other geographical representation in this paper. The authors bear the ultimate responsibility for providing appropriate place names. Views expressed in the text are those of the authors and do not necessarily reflect the views of the publisher.

Acknowledgements. Elena Kirillova and Srinivas Bikkina (Stockholm University) are acknowledged for their support during the field campaigns. We thank the technical staff at the BCOB and MCOH for their continued field support. Special thanks are due to the Maldives Meteorological Service and the government of the Republic of Maldives for their ongoing support of the joint MCOH operation. Krishnakant Budhavant expresses thanks for the additional support from the Regional Resource Centre for Asia and the Pacific (RRC.AP) at the Asian Institute of Technology (AIT), Thailand. This is Vegacenter publication number #097.

Financial support. This research was funded by the Swedish Research Council (VR Grant 2017-01601 to ÖG), the Swedish Research Council for Sustainable Development (FORMAS Grant 2023-01234 to Ö.G.). We also acknowledge the Swedish Research Council (VR) for financial support to the NordSIMS-Vegacenter national research infrastructure (Grant 2017-00671).

The publication of this article was funded by the Swedish Research Council, Forte, Formas, and Vinnova.

Review statement. This paper was edited by Eliza Harris and reviewed by two anonymous referees.

References

- Aas, W., Mortier, A., Bowersox, V., Cherian, R., Faluvegi, G., Fagerli, H., Hand, J., Klimont, Z., Galy-Lacaux, C., Lehmann, C. M. B., Myhre, C. L., Myhre, G., Olivie, D., Sato, K., Quaas, J., Rao, P. S. P., Schulz, M., Shindell, D., Skeie, R. B., Stein, A., Takemura, T., Tsyro, S., Vet, R., and Xu, X.: Global and regional trends of atmospheric sulfur, *Sci. Rep.*, 9, <https://doi.org/10.1038/s41598-018-37304-0>, 2019.
- Amrani, A., Said-Ahmad, W., Shaked, Y., and Kiene, R. P.: Sulfur isotope homogeneity of oceanic DMSP and DMS, *P. Natl. Acad. Sci. USA*, 110, <https://doi.org/10.1073/pnas.1312956110>, 2013.
- Andersson, A., Deng, J., Du, K., Zheng, M., Yan, C., Sköld, M., and Gustafsson, Ö.: Regionally-varying combustion sources of the January 2013 severe haze events over eastern China, *Environ. Sci. Technol.*, 49, <https://doi.org/10.1021/es503855e>, 2015.
- Aswini, A. R., Hegde, P., Aryasree, S., Girach, I. A., and Nair, P. R.: Continental outflow of anthropogenic aerosols over Arabian Sea and Indian Ocean during wintertime: ICARB-2018 campaign, *Sci. Total Environ.*, 712, <https://doi.org/10.1016/j.scitotenv.2019.135214>, 2020.
- Berresheim, H., Elste, T., Tremmel, H. G., Allen, A. G., Hansson, H. C., Rosman, K., Dal Maso, M., Mäkelä, J. M., Kulmala, M., and O'Dowd, C. D.: Gas-aerosol relationships of H₂SO₄, MSA, and OH: Observations in the coastal marine boundary layer at Mace Head, Ireland, *J. Geophys. Res.-Atmos.*, 107, <https://doi.org/10.1029/2000JD000229>, 2002.
- Bikkina, S., Andersson, A., Kirillova, E. N., Holmstrand, H., Tiwari, S., Srivastava, A. K., Bisht, D. S., and Gustafsson, Ö.: Air quality in megacity Delhi affected by countryside biomass burning, *Nat. Sustain.*, 2, <https://doi.org/10.1038/s41893-019-0219-0>, 2019.
- Böttcher, M. E., Brumsack, H. J., and Dürselen, C. D.: The isotopic composition of modern seawater sulfate: I. Coastal waters with special regard to the North Sea, *J. Marine Syst.*, 67, <https://doi.org/10.1016/j.jmarsys.2006.09.006>, 2007.
- Buchard, V., Randles, C. A., da Silva, A. M., Darmenov, A., Colarco, P. R., Govindaraju, R., Ferrare, R., Hair, J., Beyersdorf, A. J., Ziemba, L. D., and Yu, H.: The MERRA-2 aerosol reanalysis, 1980 onward. Part II: Evaluation and case studies, *J. Climate*, 30, <https://doi.org/10.1175/JCLI-D-16-0613.1>, 2017.
- Budhavant, K., Andersson, A., Bosch, C., Kruså, M., Murthaza, A., Zahid, and Gustafsson, Ö.: Apportioned contributions of PM_{2.5} fine aerosol particles over the Maldives (northern Indian Ocean) from local sources vs long-range transport, *Sci. Total Environ.*, 536, <https://doi.org/10.1016/j.scitotenv.2015.07.059>, 2015.
- Budhavant, K., Andersson, A., Holmstrand, H., Bikkina, P., Bikkina, S., Satheesh, S. K., and Gustafsson, Ö.: Enhanced Light-Absorption of Black Carbon in Rainwater Compared With Aerosols Over the Northern Indian Ocean, *J. Geophys. Res.-Atmos.*, 125, <https://doi.org/10.1029/2019JD031246>, 2020.
- Budhavant, K., Andersson, A., Holmstrand, H., Satheesh, S. K., and Gustafsson, Ö.: Black carbon aerosols over Indian Ocean have unique source fingerprint and optical characteristics during monsoon season, *P. Natl. Acad. Sci. USA*, 120, <https://doi.org/10.1073/pnas.2210005120>, 2023.
- Budhavant, K., Manoj, M. R., Nair, H. R. C. R., Gaita, S. M., Holmstrand, H., Salam, A., Muslim, A., Satheesh, S. K., and Gustafsson, Ö.: Changing optical properties of black carbon and brown carbon aerosols during long-range transport from the Indo-Gangetic Plain to the equatorial Indian Ocean, *Atmos. Chem. Phys.*, 24, 11911–11925, <https://doi.org/10.5194/acp-24-11911-2024>, 2024.
- Charlson, R. J., Langner, J., Rodhe, H., Leovy, C. B., and Warren, S. G.: Perturbation of the Northern Hemisphere radiative balance by backscattering from anthropogenic sulfate aerosols, *Tellus B*, 43, <https://doi.org/10.3402/tellusb.v43i4.15404>, 1991.
- Chen, B., Andersson, A., Lee, M., Kirillova, E. N., Xiao, Q., Kruså, M., Shi, M., Hu, K., Lu, Z., Streets, D. G., Du, K., and Gustafsson, Ö.: Source forensics of black carbon aerosols from China, *Environ. Sci. Technol.*, 47, <https://doi.org/10.1021/es401599r>, 2013.

- Clarke, S., Holmstrand, H., Budhavant, K., Remani, M., Haslett, S., Rodiouchkina, K., Kooyman, E., and Gustafsson, Ö.: Isotopic apportionment of sulfate aerosols between natural and anthropogenic sources in the outflow of South Asia, Bolin Centre Database [data set], <https://doi.org/10.17043/clarke-2026-sulfate-aerosols-1>, 2026.
- Dasari, S. and Widory, D.: Retrospective Isotopic Analysis of Summertime Urban Atmospheric Sulfate in South Asia Using Improved Source Constraints, *ACS ES&T Air*, 1, 357–364, <https://doi.org/10.1021/acsestair.3c00060>, 2024.
- Dasari, S., Andersson, A., Bikkina, S., Holmstrand, H., Budhavant, K., Satheesh, S., Asmi, E., Kesti, J., Backman, J., Salam, A., Bisht, D. S., Tiwari, S., Hameed, Z., and Gustafsson, Ö.: Photochemical degradation affects the light absorption of water-soluble brown carbon in the South Asian outflow, *Sci. Adv.*, 5, <https://doi.org/10.1126/sciadv.aau8066>, 2019.
- Dasari, S., Andersson, A., Stohl, A., Evangelou, N., Holmstrand, H., Budhavant, K., Salam, A., and Gustafsson, Ö.: Source Quantification of South Asian Black Carbon Aerosols with Isotopes and Modeling, *Environ. Sci. Technol.*, 54, 11771–11779, <https://doi.org/10.1021/acs.est.0c02193>, 2020.
- Elguindi, N., Granier, C., Stavrakou, T., Darras, S., Bauwens, M., Cao, H., Chen, C., Denier van der Gon, H. A. C., Dubovik, O., Fu, T. M., Henze, D. K., Jiang, Z., Keita, S., Kuenen, J. J. P., Kurokawa, J., Lioussé, C., Miyazaki, K., Müller, J. F., Qu, Z., Solmon, F., and Zheng, B.: Intercomparison of Magnitudes and Trends in Anthropogenic Surface Emissions From Bottom-Up Inventories, Top-Down Estimates, and Emission Scenarios, *Earths Future*, 8, <https://doi.org/10.1029/2020EF001520>, 2020.
- Ganguly, D., Ray, R., Majumdar, N., Chowdhury, C., and Jana, T. K.: Biogenic hydrogen sulphide emissions and non-sea sulfate aerosols over the Indian Sundarban mangrove forest, *J. Atmos. Chem.*, 75, 319–333, <https://doi.org/10.1007/s10874-018-9382-3>, 2018.
- Gelaro, R., McCarty, W., Suárez, M. J., Todling, R., Molod, A., Takacs, L., Randles, C. A., Darmenov, A., Bosilovich, M. G., Reichle, R., Wargan, K., Coy, L., Cullather, R., Draper, C., Akella, S., Buchard, V., Conaty, A., da Silva, A. M., Gu, W., Kim, G. K., Koster, R., Lucchesi, R., Merkova, D., Nielsen, J. E., Parityka, G., Pawson, S., Putman, W., Rienecker, M., Schubert, S. D., Sienkiewicz, M., and Zhao, B.: The modern-era retrospective analysis for research and applications, version 2 (MERRA-2), *J. Climate*, 30, <https://doi.org/10.1175/JCLI-D-16-0758.1>, 2017.
- Gupta, G., Ratnam, M. V., and Madhavan, B. L.: Changing patterns in the highly contributing aerosol types/species across the globe in the past two decades, *Sci. Total Environ.*, 897, <https://doi.org/10.1016/j.scitotenv.2023.165389>, 2023.
- Harris, E., Sinha, B., Van Pinxteren, D., Tilgner, A., Fomba, K. W., Schneider, J., Roth, A., Gnauk, T., Fahlbusch, B., Mertes, S., Lee, T., Collett, J., Foley, S., Borrmann, S., Hoppe, P., and Herrmann, H.: Enhanced role of transition metal ion catalysis during in-cloud oxidation of SO₂, *Science*, 340, <https://doi.org/10.1126/science.1230911>, 2013.
- Hoesly, R. M., Smith, S. J., Feng, L., Klimont, Z., Janssens-Maenhout, G., Pitkanen, T., Seibert, J. J., Vu, L., Andres, R. J., Bolt, R. M., Bond, T. C., Dawidowski, L., Kholod, N., Kurokawa, J.-I., Li, M., Liu, L., Lu, Z., Moura, M. C. P., O'Rourke, P. R., and Zhang, Q.: Historical (1750–2014) anthropogenic emissions of reactive gases and aerosols from the Community Emissions Data System (CEDS), *Geosci. Model Dev.*, 11, 369–408, <https://doi.org/10.5194/gmd-11-369-2018>, 2018.
- Jamieson, R. E. and Wadleigh, M. A.: A study of the oxygen isotopic composition of precipitation sulphate in eastern Newfoundland, *Water Air Soil Poll.*, 110, <https://doi.org/10.1023/a:1005002026009>, 1999.
- Jongebloed, U. A., Schauer, A. J., Hattori, S., Cole-Dai, J., Larrick, C. G., Salimi, S., Edouard, S. R., Geng, L., and Alexander, B.: Sulfur isotopes quantify the impact of anthropogenic activities on industrial-era Arctic sulfate in a Greenland ice core, *Environ. Res. Lett.*, 18, <https://doi.org/10.1088/1748-9326/acdc3d>, 2023.
- Keene, W. C., Pszenny, A. A. P., Galloway, J. N., and Hawley, M. E.: Sea-salt corrections and interpretation of constituent ratios in marine precipitation, *J. Geophys. Res.-Atmos.*, 91, 6647–6658, <https://doi.org/10.1029/jd091id06p06647>, 1986.
- Kesti, J., Asmi, E., O'Connor, E. J., Backman, J., Budhavant, K., Andersson, A., Dasari, S., Praveen, P. S., Zahid, H., and Gustafsson, Ö.: Changes in aerosol size distributions over the Indian Ocean during different meteorological conditions, *Tellus B*, 72, <https://doi.org/10.1080/16000889.2020.1792756>, 2020.
- Kirillova, E. N., Andersson, A., Sheesley, R. J., Kruså, M., Praveen, P. S., Budhavant, K., Safai, P. D., Rao, P. S. P., and Gustafsson, Ö.: ¹³C- And ¹⁴C-based study of sources and atmospheric processing of water-soluble organic carbon (WSOC) in South Asian aerosols, *J. Geophys. Res.-Atmos.*, 118, <https://doi.org/10.1002/jgrd.50130>, 2013.
- Kirillova, E. N., Andersson, A., Tiwari, S., Srivastava, A. K., Bisht, D. S., and Gustafsson, Ö.: Water-soluble organic carbon aerosols during a full New Delhi winter: Isotope-based source apportionment and optical properties, *J. Geophys. Res.*, 119, <https://doi.org/10.1002/2013JD020041>, 2014.
- Krishnan, R., Sabin, T. P., Vellore, R., Mujumdar, M., Sanjay, J., Goswami, B. N., Hourdin, F., Dufresne, J. L., and Terray, P.: Deciphering the desiccation trend of the South Asian monsoon hydroclimate in a warming world, *Clim. Dynam.*, 47, 1007–1027, <https://doi.org/10.1007/s00382-015-2886-5>, 2016.
- Lana, A., Bell, T. G., Simó, R., Vallina, S. M., Ballabrera-Poy, J., Kettle, A. J., Dachs, J., Bopp, L., Saltzman, E. S., Stefels, J., Johnson, J. E., and Liss, P. S.: An updated climatology of surface dimethylsulfide concentrations and emission fluxes in the global ocean, *Global Biogeochem. Cy.*, 25, <https://doi.org/10.1029/2010GB003850>, 2011.
- Lee, G., Ahn, J., Park, S. M., Moon, J., Park, R., Sim, M. S., Choi, H., Park, J., and Ahn, J. Y.: Sulfur isotope-based source apportionment and control mechanisms of PM_{2.5} sulfate in Seoul, South Korea during winter and early spring (2017–2020), *Sci. Total Environ.*, 905, <https://doi.org/10.1016/j.scitotenv.2023.167112>, 2023.
- Lelieveld, J., Pozzer, A., Pöschl, U., Fnais, M., Haines, A., and Münzel, T.: Loss of life expectancy from air pollution compared to other risk factors: A worldwide perspective, *Cardiovasc. Res.*, 116, <https://doi.org/10.1093/cvr/cvaa025>, 2020.
- Li, C., McLinden, C., Fioletov, V., Krotkov, N., Carn, S., Joiner, J., Streets, D., He, H., Ren, X., Li, Z., and Dickerson, R. R.: India Is Overtaking China as the World's Largest Emitter of Anthropogenic Sulfur Dioxide, *Sci. Rep.*, 7, <https://doi.org/10.1038/s41598-017-14639-8>, 2017.
- Li, J., Carlson, B. E., Yung, Y. L., Lv, D., Hansen, J., Penner, J. E., Liao, H., Ramaswamy, V., Kahn, R. A., Zhang, P., Dubovik,

- O., Ding, A., Lacis, A. A., Zhang, L., and Dong, Y.: Scattering and absorbing aerosols in the climate system, *Nature Reviews Earth & Environment*, <https://doi.org/10.1038/s43017-022-00296-7>, 2022.
- McDuffie, E. E., Smith, S. J., O'Rourke, P., Tibrewal, K., Venkataraman, C., Marais, E. A., Zheng, B., Crippa, M., Brauer, M., and Martin, R. V.: A global anthropogenic emission inventory of atmospheric pollutants from sector- and fuel-specific sources (1970–2017): an application of the Community Emissions Data System (CEDS), *Earth Syst. Sci. Data*, 12, 3413–3442, <https://doi.org/10.5194/essd-12-3413-2020>, 2020.
- Miyazaki, K.: TROPES Chemical Reanalysis Aerosol SO₄ 6-Hourly 3-Dimensional Product V1, NASA Goddard Earth Sciences Data and Information Services Center (GES DISC) [data set], <https://doi.org/10.5067/TWDAYANXT8UM>, 2024.
- Nair, H. R. C. R., Budhavant, K., Manoj, M. R., Andersson, A., Satheesh, S. K., Ramanathan, V., and Gustafsson, Ö.: Aerosol demasking enhances climate warming over South Asia, *NPJ Clim. Atmos. Sci.*, 6, <https://doi.org/10.1038/s41612-023-00367-6>, 2023.
- Norman, A. L., Barrie, L. A., Toom-Saunty, D., Sirois, A., Krouse, H. R., Li, S. M., and Sharma, S.: Sources of aerosol sulphate at Alert: Apportionment using stable isotopes, *J. Geophys. Res.-Atmos.*, 104, <https://doi.org/10.1029/1999JD900078>, 1999.
- Norman, A. L., Belzer, W., and Barrie, L.: Insights into the biogenic contribution to total sulphate in aerosol and precipitation in the Fraser Valley afforded by isotopes of sulphur and oxygen, *J. Geophys. Res.-Atmos.*, 109, <https://doi.org/10.1029/2002jd003072>, 2004.
- Pacific Northwest National Laboratory (PNNL): Community Emissions Data System (CEDS) version 4.21, <https://doi.org/10.25584/PNNLDataHub/1779095>, 2026.
- Ram, K., Sarin, M. M., Sudheer, A. K., and Rengarajan, R.: Carbonaceous and secondary inorganic aerosols during wintertime fog and haze over urban sites in the Indo-Gangetic plain, *Aerosol Air Qual. Res.*, 12, <https://doi.org/10.4209/aaqr.2011.07.0105>, 2012.
- Ramanathan, V., Crutzen, P. J., Lelieveld, J., Mitra, A. P., Althausen, D., Anderson, J., Andreae, M. O., Cantrell, W., Cass, G. R., Chung, C. E., Clarke, A. D., Coakley, J. A., Collins, W. D., Conant, W. C., Dulac, F., Heintzenberg, J., Heymsfield, A. J., Holben, B., Howell, S., Hudson, J., Jayaraman, A., Kiehl, J. T., Krishnamurti, T. N., Lubin, D., McFarquhar, G., Novakov, T., Ogren, J. A., Podgorny, I. A., Prather, K., Priestley, K., Prospero, J. M., Quinn, P. K., Rajeev, K., Rasch, P., Rupert, S., Sadourny, R., Satheesh, S. K., Shaw, G. E., Sheridan, P., and Valero, F. P. J.: Indian Ocean Experiment: An integrated analysis of the climate forcing and effects of the great Indo-Asian haze, *J. Geophys. Res.-Atmos.*, 106, <https://doi.org/10.1029/2001JD900133>, 2001.
- Ramarao, M. V. S., Ayantika, D. C., Krishnan, R., Sanjay, J., Sabin, T. P., Mujumdar, M., and Singh, K. K.: Signatures of aerosol-induced decline in evapotranspiration over the Indo-Gangetic Plain during the recent decades, *Mausam*, 74, 297–310, <https://doi.org/10.54302/mausam.v74i2.6031>, 2023.
- Randles, C. A., da Silva, A. M., Buchard, V., Colarco, P. R., Darmenov, A., Govindaraju, R., Smirnov, A., Holben, B., Ferrare, R., Hair, J., Shinozuka, Y., and Flynn, C. J.: The MERRA-2 aerosol reanalysis, 1980 onward. Part I: System description and data assimilation evaluation, *J. Climate*, 30, <https://doi.org/10.1175/JCLI-D-16-0609.1>, 2017.
- Rastogi, N., Agnihotri, R., Sawlani, R., Patel, A., Babu, S. S., and Satish, R.: Chemical and isotopic characteristics of PM₁₀ over the Bay of Bengal: Effects of continental outflow on a marine environment, *Sci. Total Environ.*, 726, <https://doi.org/10.1016/j.scitotenv.2020.138438>, 2020.
- Rees, C. E., Jenkins, W. J., and Monster, J.: The sulphur isotopic composition of ocean water sulphate, *Geochim. Cosmochim. Ac.*, 42, [https://doi.org/10.1016/0016-7037\(78\)90268-5](https://doi.org/10.1016/0016-7037(78)90268-5), 1978.
- Rodiouchkina, K.: Development of a multi-collector inductively coupled plasma massspectrometry method for measurement of stable sulphur isotope ratios in aerosol sulphate, MS thesis Uppsala University, <https://urn.kb.se/resolve?urn=urn:nbn:se:uu:diva-357614> (last access: 23 February 2026), 2018.
- Sawlani, R., Agnihotri, R., Sharma, C., Patra, P. K., Dimri, A. P., Ram, K., and Verma, R. L.: The severe Delhi SMOG of 2016: A case of delayed crop residue burning, coincident firecracker emissions, and atypical meteorology, *Atmos. Pollut. Res.*, 10, <https://doi.org/10.1016/j.apr.2018.12.015>, 2019.
- Seguin, A. M., Norman, A. L., Eaton, S., Wadleigh, M., and Sharma, S.: Elevated biogenic sulphur dioxide concentrations over the North Atlantic, *Atmos. Environ.*, 44, 1139–1144, <https://doi.org/10.1016/j.atmosenv.2010.01.005>, 2010.
- Seguin, A. M., Norman, A. L., Eaton, S., and Wadleigh, M.: Seasonality in size segregated biogenic, anthropogenic and sea salt sulfate aerosols over the North Atlantic, *Atmos. Environ.*, 45, <https://doi.org/10.1016/j.atmosenv.2011.09.033>, 2011.
- Sharma, S. and Kumar, A. (Eds.): Air pollutant emissions scenario for India – Version 1, The Energy and Resources Institute, New Delhi, India, ISBN 978-81-7993-639-9, 2016.
- Shenoy, D. M. and Kumar, M. D.: Variability in abundance and fluxes of dimethyl sulphide in the Indian Ocean, *Biogeochemistry*, <https://doi.org/10.1007/s10533-007-9092-4>, 2007.
- Szopa, S., Naik, V., Adhikary, B., Artaxo, P., Bernsten, T., Collins, W. D., Aas, W., Akritidis, D., Allen, R. J., Kanaya, Y., Prather, M. J., Kuo, C., Zhai, P., Pirani, A., Connors, S., Péan, C., Berger, S., Caud, N., Chen, Y., Goldfarb, L., Gomis, M., Huang, M., Leitzell, K., Lonnoy, E., Matthews, J., Maycock, T., Waterfield, T., Yelekçi, O., Yu, R., and Zhou, B.: Short-Lived Climate Forcers. In: *Climate Change 2021: The Physical Science Basis. Contribution of Working Group I to the Sixth Assessment Report of the Intergovernmental Panel on Climate Change*, Cambridge University Press, <https://doi.org/10.1017/9781009157896.008>, 2021.
- Verma, S., Boucher, O., Shekar Reddy, M., Upadhyaya, H. C., Le Van, P., Binkowski, F. S., and Sharma, O. P.: Tropospheric distribution of sulphate aerosols mass and number concentration during INDOEX-IFP and its transport over the Indian Ocean: a GCM study, *Atmos. Chem. Phys.*, 12, 6185–6196, <https://doi.org/10.5194/acp-12-6185-2012>, 2012.
- Wadleigh, M. A.: Sulphur isotopic composition of aerosols over the western North Atlantic Ocean, *Can. J. Fish. Aquat. Sci.*, <https://doi.org/10.1139/F04-073>, 2004.
- Winiger, P., Andersson, A., Yttri, K. E., Tunved, P., and Gustafsson, Ö.: Isotope-Based Source Apportionment of EC Aerosol Particles during Winter High-Pollution Events at the Zeppelin Observatory, Svalbard, *Environ. Sci. Technol.*, 49, <https://doi.org/10.1021/acs.est.5b02644>, 2015.

World Health Organization: WHO global air quality guidelines: particulate matter (PM_{2.5} and PM₁₀), ozone, nitrogen dioxide, sulfur dioxide and carbon monoxide, World Health Organization, 2021, <https://www.who.int/publications/item/9789240034228> (last access: 9 April 2026), 2021.